

RSC Advances



This is an *Accepted Manuscript*, which has been through the Royal Society of Chemistry peer review process and has been accepted for publication.

Accepted Manuscripts are published online shortly after acceptance, before technical editing, formatting and proof reading. Using this free service, authors can make their results available to the community, in citable form, before we publish the edited article. This *Accepted Manuscript* will be replaced by the edited, formatted and paginated article as soon as this is available.

You can find more information about *Accepted Manuscripts* in the [Information for Authors](#).

Please note that technical editing may introduce minor changes to the text and/or graphics, which may alter content. The journal's standard [Terms & Conditions](#) and the [Ethical guidelines](#) still apply. In no event shall the Royal Society of Chemistry be held responsible for any errors or omissions in this *Accepted Manuscript* or any consequences arising from the use of any information it contains.

Synthesis and self-assembly of hierarchical SiO₂-QDs@SiO₂ nanostructures and their photoluminescence applications for fingerprint detecting and cell imaging

Wenjun Dong^{1*}, Yan Cheng¹, Liang Luo¹, Xiaoyun Li¹, Lina Wang¹, Chunguang Li², Lifeng Wang^{3*}

¹ Center for Nanoscience and Nanotechnology, Zhejiang Sci-Tech University, Hangzhou 310018, China

² State Key Laboratory of Inorganic Synthesis and Preparative Chemistry, College of Chemistry, Jilin University, Changchun 130012, China

³ School of Aeronautics Science and Engineering Beijing University of Aeronautics and Astronautics Beijing 100191 China.

Abstract

Hierarchical SiO₂-QDs@SiO₂ (QDs=CdTe, PbTe or PbS) nanostructures have been prepared by an integrated synthesis and self-assembly strategy using 3-mercaptopropionic acid (MPA) to stabilize the QDs and NaOH to control the self-assembly of QDs on the SiO₂ nanobead carriers. 3-10 nm QDs covered with a 1-2 nm SiO₂ shells were embedded on the surface of 50 nm SiO₂ nanobead carriers separately, resulting in hierarchical SiO₂-QDs@SiO₂ nanostructures. MPA and NaOH played important roles in the nucleation and growth of QDs, etching the SiO₂ nanobead carriers to colloidal surface, and self-assembly of the QDs on viscous SiO₂ nanobead carriers. The hierarchical SiO₂-QDs@SiO₂ nanostructures possess various advantages: (I) the growth of QDs and self-assembly of QDs on SiO₂ nanobead carriers were performed in a one-pot reaction by a facile aqueous phase refluxing approach; (II) the SiO₂ shell with 1-2 nm in thickness can prevent the leakage of toxic Cd²⁺ or Pb²⁺ and avoid photobleaching or environmental pollution; (III) the surface of hierarchical SiO₂-QDs@SiO₂ nanostructures can be functionalized easily through silane-coupling chemistry. Due to the excellent photoluminescence and biocompatibility, the hierarchical SiO₂-QDs@SiO₂ nanostructures modified by carboxyl (-COOH) active group can be available for covalent coupling to various biomolecules, which have shown potential applications in fingerprint detecting and in vivo cell imaging.

Keywords: SiO₂-QDs@SiO₂, hierarchical nanostructures, fingerprint detecting, cell imaging

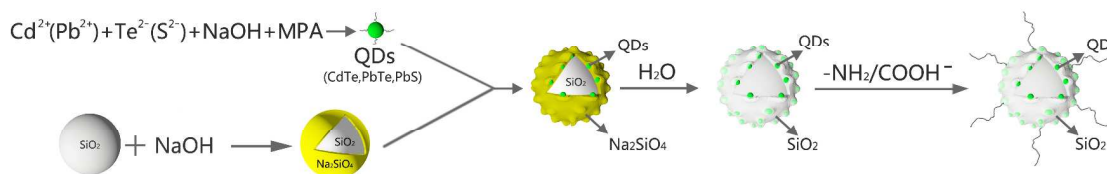
* E-mail: wenjundong@zstu.edu.cn (W. Dong), wanglifeng@ase.buaa.edu.cn (L. Wang)

1. Introduction

Due to the unique size-tunable, narrow emission and high photostability properties, semiconductor quantum dots (QDs) have been attracting extensive attention [1-3], such as light-emitting diode [4-5], vivo imaging [6-7], optoelectronic and photovoltaic devices [8-10]. However, QDs were susceptible to external environment and easy to lose their fluorescence due to the optical and chemical instability in harsh environment. On the other hand, QDs generally contain highly toxic heavy metal ions such as Cd^{2+} , Pb^{2+} , which are easy to cause environmental pollution [11-12]. Up to now, a series of stable coating such as polymer and silica have been developed to improve the chemical stability and biocompatibility of the QDs. Silica coating, as a popular inert material, can provide chemical/physical shielding from the direct environment and possess good water dispersibility [13-15]. Moreover, the surface of QDs with silica coating can be easily modified by various functional groups through silane-coupling method [16]. For example, Rogach et al encapsulated luminescent QDs into the SiO_2 particles by the Stöber method, and the QDs@ SiO_2 core-shell nanocomposites showed good biocompatibility and photostability for fluorescence imaging [17]. Emilio et al encapsulated QDs in SiO_2 nanoparticles via the reverse microemulsion methodology, and the obtained multiplexed colored silica-QDs nanohybrids could avoid quenching of the photoluminescence (PL) of QDs [18]. These coating methods for preparing QDs involved complicated steps and non-environmental solvent, so exploring a simple green method to prepare QDs with high photostability still remains as a challenge.

In this paper, an integrated synthesis and self-assembly strategy for preparing the hierarchical SiO_2 -QDs@ SiO_2 (QDs=CdTe, PbTe or PbS) nanostructures in aqueous solution has been developed. The growth of QDs and self-assembly process were involved in this one-pot synthesis. The fabrication of hierarchical SiO_2 -QDs@ SiO_2 nanostructures, which was include the synthesis of 3-10 nm QDs and self-assembly of QDs on the SiO_2 nanobead carriers in a

one-pot reaction. Fortunately, the hierarchical $\text{SiO}_2\text{-QDs@SiO}_2$ nanostructures can be successfully modified by $-\text{COOH}$ or $-\text{NH}_2$ active group by the silane-coupling agent, and then the functionalized hierarchical nanostructures ($\text{SiO}_2\text{-QDs@SiO}_2\text{-COOH}$ or $\text{SiO}_2\text{-QDs@SiO}_2\text{-NH}_2$) can be obtained. The as-prepared multicolored hierarchical $\text{SiO}_2\text{-CdTe@SiO}_2\text{-COOH}$ nanostructures have strong binding affinity for amino acids of the fingerprint by cross-coupling reaction, which can be available for making the fingerprint images visualized without background influence [19]. On the other hand, the as-obtained multicolored hierarchical $\text{SiO}_2\text{-CdTe@SiO}_2\text{-COOH}$ nanostructures show high PL fluorescence and good biocompatibility which could be effective for the enhancement of cell bioimaging. The synthetic process of the $\text{SiO}_2\text{-QDs@SiO}_2$ nanostructure is schematic representation in Scheme 1.



Scheme 1. Synthetic procedures of the hierarchical $\text{SiO}_2\text{-QDs@SiO}_2$ nanostructure.

2. Experimental details

All chemicals used in this work were of analytical grade without further purification, and the reactions were carried out under open-air conditions. Tetrabutyl titanate, cadmium chloride hydrate ($\text{CdCl}_2 \cdot 2.5\text{H}_2\text{O}$, 99%), tetraethoxysilane (TEOS), triton X-100, succinic anhydride (95%), 1-hexanol (98%), ammonia, sodium tellurite (97%), hydrazine hydrate, toluene, N,N-Dimethylformamide (DMF), (3-Aminopropyl)-triethoxysilane AMEO (KH550), 3-mercaptopropionic acid (MPA, $\text{C}_3\text{H}_6\text{O}_2\text{S}$, 99%), sodium sulphide, lead acetate and cyclohexane (98%) were purchased from Aladdin Chemistry Co., Shanghai, China.

The morphology of the hierarchical $\text{SiO}_2\text{-QDs@SiO}_2$ nanostructures were investigated by field emission scanning electron microscopy (FESEM, Hitachi S-4800, Japan) and transmission

electron microscopy (TEM, JEM-2100, Japan). The elemental compositions of the SiO₂-QDs@SiO₂ were confirmed via spatially energy dispersive X-ray spectroscopy (EDS, Falcon, EDAX). The X-ray diffraction (XRD) pattern of the SiO₂-CdTe@SiO₂ was recorded on a Bruker AXS D8 Discover diffraction system with a Cu K α -radiation source ($\lambda=1.5406 \text{ \AA}$) at a scanning rate of 0.02 °/s in the 2θ range of 10°-60°. FT-IR spectra of the surface functionalization of SiO₂-CdTe@SiO₂ were carried out using KBr tablets (1% w/w of product in KBr) with a resolution of 4 cm⁻¹ and 100 scans per sample.

Synthesis of hierarchical SiO₂-QDs@SiO₂ (QDs=CdTe, PbTe or PbS) nanostructures

1.(i)Synthesis of hierarchical SiO₂-CdTe@SiO₂ nanostructures with the PL emission from yellow to red. In a typical procedure, 0.1 g of the SiO₂ nanobead carriers (prepared as the reference [20]) were added into a flask containing 48.0 mL of deionized water, 40 μ L of MPA and 1.6 mL of 0.1M CdCl₂ solution. The pH value of the solution was adjusted to 10.0 by 0.1M of NaOH solution, and 8.0 mg of Na₂TeO₃ were added into the solution and stirred for 6 h at 80 °C. Subsequently 1.0 mL of 80% hydrazine hydrate was added into the solution. Series of hierarchical SiO₂-CdTe@SiO₂ nanostructures with different colors from yellow to dark red could be obtained by adjusting the period of the refluxing time.

(ii)Synthesis of hierarchical SiO₂-CdTe@SiO₂ nanostructures with green PL emission. The NaHTe, an intermediate product for preparation of CdTe QDs, was firstly synthesized by the reduction of tellurium powder with NaBH₄ [21]. In a typical procedure, 45 mg of NaBH₄, 16 mg of Te powder and 2 mL of deionized water were added into a flasket, and then kept the flasket in 60 °C water bath for several minutes until the black Te powder was disappeared. Then, the white sodium tetraborate (Na₂B₄O₇) precipitate appeared on the bottom of the flasket and cooled the flasket by ice. The synthesis process of hierarchical SiO₂-CdTe@SiO₂ nanostructures was as following: 30 mL of solution containing 84.5 mg of CdCl₂, 60 μ L of MPA and 0.1 g of SiO₂ nanobead carriers were transferred into a flask, and the pH value of the solution was adjusted to

10.0 by 0.1 M of NaOH solution and purged with N₂ for 1 h. Subsequently, 1.2 mL of oxygen-free NaHTe aqueous solution was injected into the solution, and refluxed at 100 °C for 1 h. The orange products were centrifuged at 5000rp for 5 min and washed with ethanol and deionized water for three times, respectively. Then the hierarchical SiO₂-CdTe@SiO₂ nanostructures were obtained.

2. *Synthesis of hierarchical SiO₂-PbTe (PbS)@SiO₂ nanostructures with the Near-IR PL emission.* The hierarchical SiO₂-PbTe@SiO₂ or SiO₂-PbS@SiO₂ nanostructures could be synthesized with similar recipe by using (CH₃COO)₂Pb as Pb source and NaTeO₃ or Na₂SO₃ as Te or S source. 0.1 g of the SiO₂ nanobead carriers were added into a flask containing 48.0 mL of deionized water, 40 μL of MPA and 1.6 mL of 0.1M (CH₃COO)₂Pb solution. The pH value of the solution was adjusted to 10.0 by 0.1M of NaOH solution, and 8.0 mg of Na₂TeO₃ were added into the solution and stirred for 6 h at 80 °C. Subsequently 1.0 mL of 80% hydrazine hydrate was added into the solution. Series of hierarchical SiO₂-PbTe (PbS)@SiO₂ nanostructures with different sizes with the Near-IR PL emission could be obtained by adjusting the period of the refluxing time.

Modification of the hierarchical SiO₂-CdTe@SiO₂ nanostructures by -COOH or -NH₂ groups.

As we know, the -OH group of Si-OH on the surface of SiO₂-CdTe@SiO₂ nanostructures can conjugated to other active groups through the silane-coupling reaction, and then -COOH or -NH₂ functional group modified SiO₂-CdTe@SiO₂ nanostructures can be obtained.

(i) Modification of the hierarchical SiO₂-CdTe@SiO₂ nanostructures by -COOH group: Typically, 0.1 g of succinic anhydride, 25 mL of N,N-Dimethylformamide (DMF) and 235 μL of KH550 were transferred into a flask, and kept at 70 °C for 3 h to obtain the -COOH group conjugated KH550 (KH550-COOH). Subsequently, 0.1 g of the hierarchical SiO₂-CdTe@SiO₂ nanostructures was added into the KH550-COOH solution to obtain the hierarchical SiO₂-CdTe@SiO₂-COOH nanostructures. Finally, the resulting products were centrifuged at

5000rp for 5 min and washed with ethanol and water for three times, respectively. The samples were redisperses in deionized water as a stock solution.

(ii) Modification of the hierarchical $\text{SiO}_2\text{-CdTe@SiO}_2$ nanostructures by $-\text{NH}_2$ group: Typically, 0.1 g of the hierarchical $\text{SiO}_2\text{-CdTe@SiO}_2$ nanostructures, 10.0 mL of toluene and 700 μL of KH550 were transferred into a flask, and refluxed at 80 °C for 12 h to obtain the hierarchical $\text{SiO}_2\text{-CdTe@SiO}_2\text{-NH}_2$ nanostructures. Finally, the resulting products were centrifuged at 5000rp for 5 min and washed with ethanol and deionized water for three times, respectively. The samples were redispersed in deionized water as a stock solution.

Fingerprint detecting test. Fingerprinted on a clean glass substrate, and then painted the solution of $\text{SiO}_2\text{-CdTe@SiO}_2$ that containing carboxyl on the glass uniformly and air drying for two hours. After washing with deionized water, place the glass substrate under the UV light.

Cell imaging experiment. The potential bioimaging application of hierarchical $\text{SiO}_2\text{-CdTe@SiO}_2\text{-COOH}$ nanostructures were carried out on the HeLa cells. First, the HeLa cells were grown in Dulbecco's Modified Eagle Medium supplemented with 5% fetal bovine serum and 1% antibiotics at 37°C and 5% CO_2 , then seeded in 96-well tissue culture plates and allowed to adhere for 5 h. Subsequently, after washing with phosphate-buffered saline solution, the HeLa cells were incubated in a serum-free medium that contained hierarchical $\text{SiO}_2\text{-CdTe@SiO}_2\text{-COOH}$ nanostructures at 37 °C for 3 h under 5% CO_2 .

MTT assay. HeLa cells were cultured in Dulbecco's Modified Eagles Medium (DMEM) supplemented with 10% fetal bovine serum (FBS) and antibiotics (100 U/ml penicillin, 100 mg/ml streptomycin). The SiO_2 , $\text{SiO}_2\text{-QDs@SiO}_2$ and QDs solutions with culture medium containing HeLa cells were cultured in an humidified incubator with 5% CO_2 at 37 °C. Cell viability was evaluated by using a 3-(4,5-dimethylthiazol-2-yl)-2,5-diphenyl tetrazolium bromide (MTT; Sigma) reduction conversion assay and cell survival was expressed as

absorbance at 570 nm in a spectrophotometric microplate reader (Bio-RAD Model 680, USA).

3. Results and discussion

3.1. Morphology and structures

Fig.1 shows the SEM images of the as-prepared SiO₂ nanobead carriers, hierarchical SiO₂-CdTe@SiO₂, SiO₂-PbTe@SiO₂, SiO₂-PbS@SiO₂, SiO₂-CdTe@SiO₂-COOH and SiO₂-CdTe@SiO₂-NH₂ nanostructures. The as-prepared SiO₂ nanobead carriers are generally spherical shape and uniform (as shown in Fig.1a). The morphology of hierarchical SiO₂-CdTe@SiO₂ nanostructures shows that the small CdTe QDs are coated onto the surface of SiO₂ nanobead carriers (as shown in Fig.1b). The corresponding EDAX spectrum demonstrates the presence of Cd, Te, Si and O element in the final products (as shown in the inset one of Fig.1b). Hierarchical SiO₂-PbTe@SiO₂ and SiO₂-PbS@SiO₂ nanostructures can be successfully synthesized when (CH₃COO)₂Pb as Pb source and NaTeO₃ (Na₂SO₃) as Te (S) source. The hierarchical SiO₂-PbTe@SiO₂ and SiO₂-PbS@SiO₂ nanostructures show similar morphology as that of SiO₂-CdTe@SiO₂ nanostructures (as shown in Fig.1 c and d). The chemical properties of the surface of nanostructures can be modified through conjugation of the active groups, and the SEM images confirmed that the morphology of hierarchical SiO₂-CdTe@SiO₂-COOH and SiO₂-CdTe@SiO₂-NH₂ still remains as the original (as shown in Fig. 1e and f).

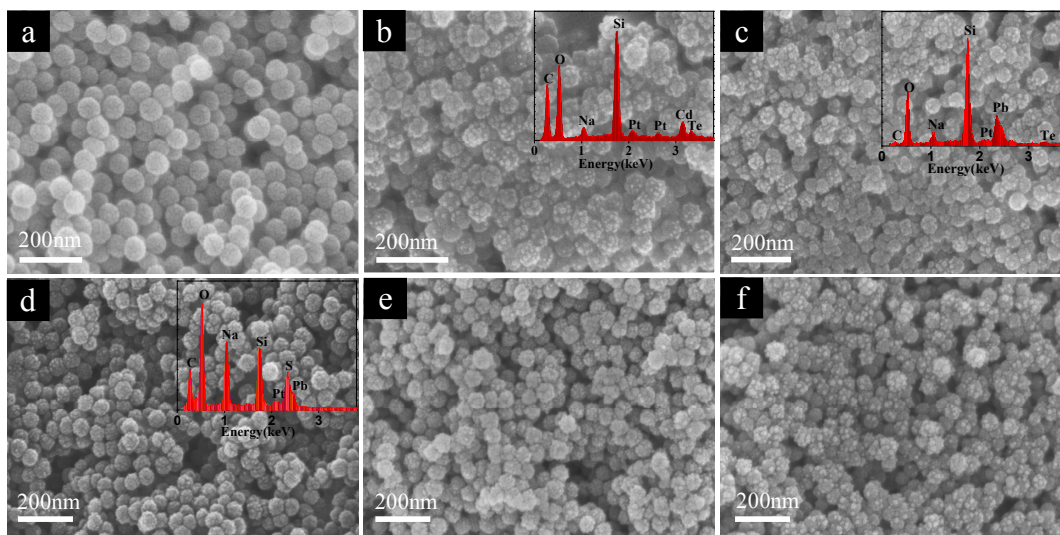


Figure 1 SEM images of (a) SiO₂, (b) SiO₂-CdTe@SiO₂, (c) SiO₂-PbTe@SiO₂, (d) SiO₂-PbS@SiO₂, (e) SiO₂-CdTe@SiO₂-COOH, and (f) SiO₂-CdTe@SiO₂-NH₂. Insets of Fig.1b, c and d show the corresponding EDAX of hierarchical SiO₂-CdTe@SiO₂, SiO₂-PbTe@SiO₂ and SiO₂-PbS@SiO₂ nanostructures

HRTEM characterization was applied to investigate the structure and morphology of the QDs of the hierarchical SiO₂-QDs@SiO₂ nanostructures. TEM images of QDs depicts that 3-10 nm QDs covered by a 1-2 nm SiO₂ shells were embedded onto the surface of the SiO₂ nanobead carriers (as shown in Fig.2). The uniform CdTe QDs about 5 nm in diameter deposited onto the surface of SiO₂ nanobead carriers with approximately 50 nm in diameter were separated well (as shown in Fig.2a). The HRTEM image of a CdTe QDs shows that the QDs is well-crystallized, and the lattice fringe with spacing of approximately 0.34 nm is corresponded to the interplanar distance of the (200) plane in the cubic CdTe (JCPDS Card No. 65-1046) (as shown in Fig.2b). The PbTe QDs with 7 nm in diameter were separated well onto the surface of SiO₂ nanobead carriers (as shown in Fig.2c). The PbTe QDs covered by a 2 nm of SiO₂ shell was embedded on the surface of SiO₂ nanobead carriers (as shown in Fig.2d). In addition, the HRTEM image of PbTe QDs shows that *d* value of a PbTe QDs is about 0.33 nm, which can be assigned to the (200) reflection of cubic PbTe (as shown in Fig.2d). Similarly, the PbS QDs with a diameter of about 6

nm are deposited onto the surface of SiO₂ nanobead carriers separately (as shown in Fig.2e). HRTEM image of the hierarchical SiO₂-PbS@SiO₂ nanostructures shows that *d* value of the PbS QDs is approximately 0.32 nm, which is corresponded to the (111) plane of cubic PbS (as shown in Fig.2f).

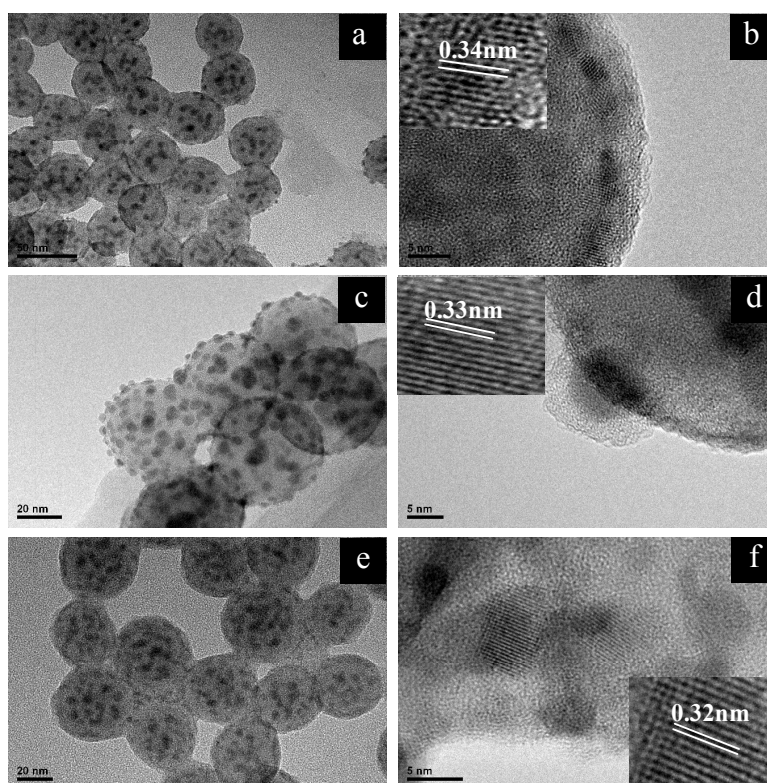


Figure 2 TEM images of hierarchical SiO₂-CdTe@SiO₂ (a, b), SiO₂-PbTe@SiO₂ (c, d), and SiO₂-PbS@SiO₂ (e, f) nanostructures. The inserts of Fig.2b, d and f show the representative HRTEM image.

The growth of QDs and self-assembly of QDs and SiO₂ nanobead carriers are two important steps towards generating the advanced hierarchical SiO₂-QDs@SiO₂ nanostructures. In the synthesis process, MPA and NaOH have played important roles in the synthesis and self-assembly strategy and then the formation of the hierarchical SiO₂-QDs@SiO₂ nanostructures. MPA, acting as the stabilizer, is a superior capping molecule for producing stable QDs and the carboxylic groups of MPA may coordinate with the Cd or Pb site of monomers or

clusters for fast growth of QDs nanocrystal. On the other hand, NaOH is another agent influencing the formation of hierarchical SiO₂-QDs@SiO₂ nanostructures [22]. NaOH can favor the PL enhancement in the colloid solution by decreasing the defects attributed to the formation of Cd-thiol (Cd(SR)) complexes on CdTe QDs surfaces. Furthermore, NaOH can assist the self-assembly of QDs on the surface of SiO₂ nanobead carriers, which include the following sequence: from (i) etching the surface of SiO₂ nanobead carriers by NaOH solution to obtain the colloidal surface to; (ii) adhering QDs on the viscous surface of SiO₂ nanobead carriers to; (iii) covering the QDs by a colloidal SiO₂ shell and then (iv) forming the hierarchical SiO₂-QDs@SiO₂ nanostructures.

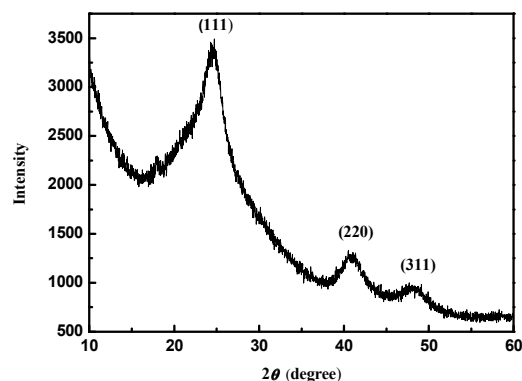


Figure 3 XRD patterns of the hierarchical SiO₂-CdTe@SiO₂ nanostructures

X-ray diffraction analysis was applied to investigate the CdTe crystalline of hierarchical SiO₂-CdTe@SiO₂ nanostructures. Three broad peaks at about 24.5°, 40.5° and 48° are correspond to the (111), (220), and (311) planes, which are matched with the cubic zinc blende structure of CdTe crystal (as shown in Fig.3). According to the XRD data, the average QDs size can be quantitatively evaluated using the Debye-Scherrer formula relates, which gives the relationship between peak broadening in the XRD and particle size:

$$D = 0.89\lambda / (B_{size} \cos\theta_B)$$

Where 0.89 is the Debye-Scherrer constant, λ represents the X-ray wavelength ($\lambda=1.5406 \text{ \AA}$),

B_{size} is the full width at half-maximum and θ_B is the Bragg diffraction angle [23]. The nanoparticle size of CdTe QDs determined by the Debye-Scherrer equation is about 4.5 nm, which is corresponded to the information obtained from the HRTEM image of CdTe QDs (as shown in Fig.2a).

3.2. Characterization of surface functionalization

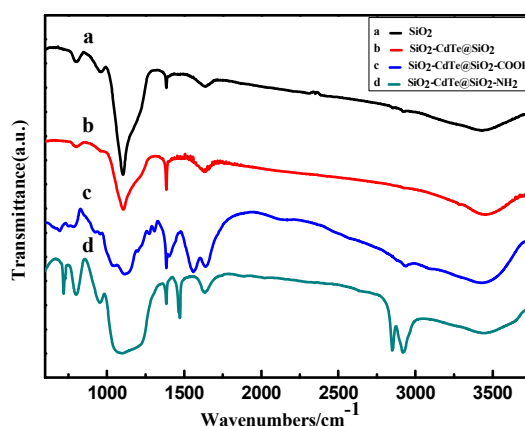


Figure 4 FT-IR spectra of (a) SiO₂, (b) SiO₂-CdTe@SiO₂, (c) SiO₂-CdTe@SiO₂-COOH and (d) SiO₂-CdTe@SiO₂-NH₂ (samples a-d)

As we know, most applications of QDs are directly dependent on the chemistries that make them hydrophilic and biofunctional. The hierarchical SiO₂-CdTe@SiO₂-COOH or SiO₂-CdTe@SiO₂-NH₂ nanostructures give a chemical link with various functional molecules for promising applications. In this paper, the hierarchical SiO₂-CdTe@SiO₂-COOH nanostructures can pave the way for applying them in the fields of imaging vivo cells and detecting fingerprint. FT-IR spectra are applied to confirm the surface binding of capping groups. The IR spectra of the samples confirmed -COOH or -NH₂ group were successfully connected to the hierarchical SiO₂-CdTe@SiO₂ nanostructures. The FT-IR spectra of hierarchical SiO₂-CdTe@SiO₂-COOH confirms that the successful functionalization of hierarchical SiO₂-CdTe@SiO₂ by the presence of carbonyl group (-CO-, $\nu_{C=O} \approx 1565 \text{ cm}^{-1}$) and hydroxyl group (-OH, $\nu_{O-H} \approx 3448 \text{ cm}^{-1}$) [24], as shown in Fig.4c. In addition, FT-IR spectra confirms the

amino group ($-\text{NH}_2$) is also successfully connected to the hierarchical $\text{SiO}_2\text{-CdTe@SiO}_2$ by the presence of peaks at about 1470 , 2580 and 2924 cm^{-1} [25] (as shown in Fig.4d). Two distinct peaks for the SiO_2 nanobead carriers at about 800 and 1100 cm^{-1} are attributed to the symmetric contraction vibration peak at horizontal and vertical of the bond of Si-O-Si. The presence of 1385 cm^{-1} is due to the interaction of the samples with the KBr in the tablets, and the band around 1635 cm^{-1} is assigned to the bending mode of the interlayer water molecule [26].

3.3. Optical properties of the hierarchical $\text{SiO}_2\text{-CdTe@SiO}_2$ nanostructures

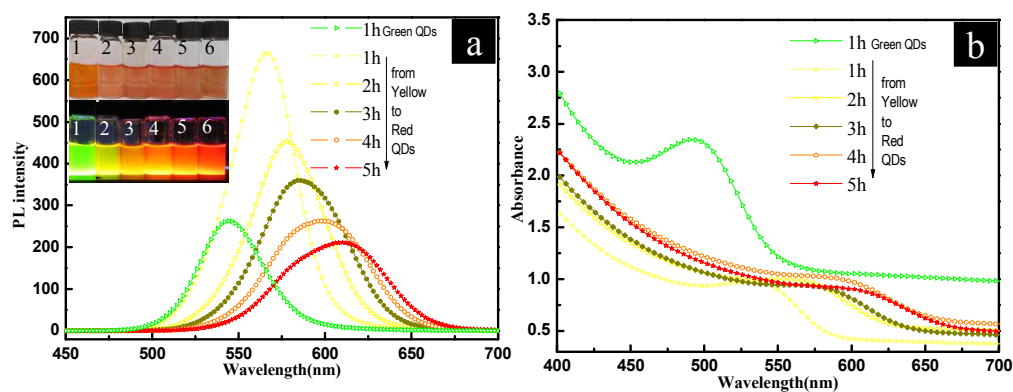


Figure 5 Emission (a) and absorption (b) spectra of hierarchical $\text{SiO}_2\text{-CdTe@SiO}_2$ nanostructures in aqueous solution (excitation wave length: 380 nm), colloidal solutions of hierarchical $\text{SiO}_2\text{-CdTe@SiO}_2$ nanostructures (left to right, inserts of Fig. 4b) consisting of samples 1-6 obtained by the aforementioned methods under normal and UV light (352 nm , 6 W)

It is well known that the PL wavelength range of QDs can be finely tuned by changing the size of the QDs particles [27-28]. In this paper, hierarchical $\text{SiO}_2\text{-CdTe@SiO}_2$ nanostructures show excellent luminescence properties and the PL colors can be tuned from green to red in the visible spectrum. Figure 5 shows the PL spectra, normalized UV-vis absorption spectra and corresponding photographs of the solution of hierarchical $\text{SiO}_2\text{-CdTe@SiO}_2$ nanostructures. The PL emission peaks of CdTe QDs range from 535 nm to 640 nm , which reveals the tunable emission spectrum is in the visible range (as shown in Fig.5a). The size-dependent quantum

confinement effects are apparent during the CdTe QDs growth process as solutions in vials shift across the visible spectrum from green to red emission (as shown in inset of Fig.5b). The corresponding peak position in UV-vis spectra ranges from 460 nm to 610 nm attributed to the increase in the non-radiative recombination of electrons and holes on the surface of the CdTe QDs as the size increases [29]. During the growth of CdTe QDs, smaller particles will dissolve and become the constituents of larger QDs, a process known as Ostwald ripening. The tunable colors of the hierarchical $\text{SiO}_2\text{-CdTe@SiO}_2$ nanostructures implies that our facile method can control the size of CdTe QDs from 2.6 nm to 5.0 nm, as a result that the PL emission from green to red region of the visible spectrum. Interestingly, the hierarchical $\text{SiO}_2\text{-CdTe@SiO}_2$ nanostructures still remains its PL properties after the modification by $-\text{COOH}$ or $-\text{NH}_2$ group. The SiO_2 coating prevents the oxidative and photothermal degradation of the QDs and increases the stability of QDs@SiO_2 nanostructures. The spectra of $\text{SiO}_2\text{-CdTe @SiO}_2$ nanostructures exhibit only a slight red shift (~ 25 meV) over 30 days of water soaking and almost zero peak broadening for 60 days in air.

4. Fingerprint detecting

The pattern of friction ridge skin on the finger of the hands is unique to each individual, which can provide significantly information about one person [30-32]. Usually, ninhydrin solution, iodine/benzoflavone spray [33] and vacuum metal deposition [34] techniques have been developed to detect the fingerprint. However, these methods suffered from being influenced by the complex background. QDs can luminesce with great intensity and high photostability than commercially available organic fluorescence dyes, and so the QDs are the potentially ideal reagents for detecting the latent fingerprint deposited on polychrome substance. For instance,

Sametband et al. have shown that CdSe/ZnS QDs stabilized with n-alkaneamines in the organic solution can be used for the direct visualization of latent fingerprint on wet nonporous surfaces [35]. CdS/dendrimer in organic solvent has also been used for the detection of fingerprint [36-37]. However, the toxicity of QDs without protecting shell may hinder their applications in the fields of fingerprint detecting. Fortunately, the hierarchical $\text{SiO}_2\text{-CdTe@SiO}_2\text{-COOH}$ nanostructures demonstrate forensic work on the fingerprint detecting.

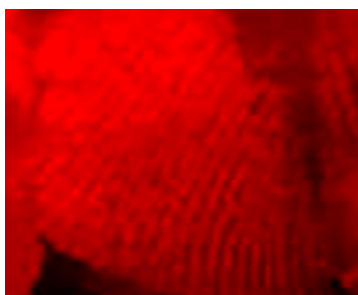


Figure 6 Photographs of the detection of a fingerprint deposited the glass under UV light (352 nm, 6 W)

Hierarchical $\text{SiO}_2\text{-CdTe@SiO}_2\text{-COOH}$ nanostructures can interact with the amino acid of a fingerprint, especially the sebum-rich fingerprint, and so acts as a dusting powder to locate and visualize fingerprints under the UV light [38]. Because the emission of the multicolored CdTe QDs in aqueous solution under UV light covers almost the visible region from green to red, the fingerprint deposited on objects can be readily detected without being influenced by the background colors. A fingerprint on the glass substrate was detected by the hierarchical $\text{SiO}_2\text{-CdTe@SiO}_2\text{-COOH}$ nanostructures, and the fluorescence photographs were shown in the figure 6. The -COOH groups modified on the hierarchical $\text{SiO}_2\text{-CdTe@SiO}_2\text{-COOH}$ nanostructures has a strong affinity for the amino acid or grease in the substances of the fingerprint, thereby enabling the visualization of the fingerprint, even the prints are faint.

5. Cells imaging

The free carboxyl (-COOH) group conjugated on the surface of hierarchical $\text{SiO}_2\text{-CdTe@SiO}_2\text{-COOH}$ nanostructures is available for covalent coupling to various

biomolecules (such as proteins, peptides and nucleic acids) by cross-linking to reactive amine (-NH₂) groups of the vivo cells. The luminescence images of HeLa cells were shown in Figure 7. The bright spots are attributed to the CdTe QDs of the hierarchical SiO₂-CdTe@SiO₂-COOH nanostructures, which can illuminate the entire image of the cell (as shown in Fig.7a and c). The cell image could also demonstrate by the dark frame (Fig.7b). These bright spots are mainly distributed in the membrane of HeLa cells. The shape and position of HeLa cells (as shown in Fig.7a and c) indicate the strong interaction between HeLa cells and hierarchical SiO₂-CdTe@SiO₂-COOH nanostructures by forming the covalent bonds. It is obvious that the hierarchical SiO₂-CdTe@SiO₂-COOH nanostructures did not permeate the cytomembrane, rendering the hierarchical SiO₂-CdTe@SiO₂-COOH nanostructures suitable for cell-labeling markers.

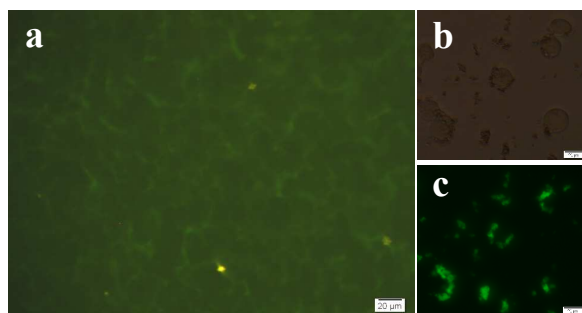


Figure 7 Fluorescence imaging of HeLa cells after incubated with hierarchical SiO₂-CdTe@SiO₂-COOH nanostructures (green-emitting nanocrystals). The acquisition was performed using the continuous-wave laser source emitting at 380 nm.

The quantity of the living cells was reflected by MTT assays (Figure 8). The MTT results reveal that SiO₂ shell increased cellular proliferation without any evidence of cytotoxicity and the viability of HeLa cells were similar to the results of the SiO₂ control test, while the QDs without SiO₂ shell had obvious cytotoxicity. After 7 days cultured, the number of living cells decline dramatically.

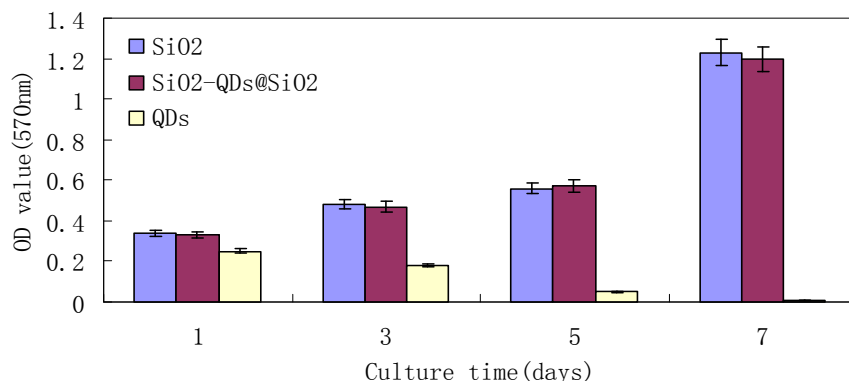


Figure 8 Comparison of the proliferation and of HeLa cells cultured with SiO₂, SiO₂-QDs@SiO₂ and QDs solutions after 1, 3, 5 and 7 days of culture, respectively.

6. Conclusion

In general, an integrated synthesis and self-assembly strategy for preparing the hierarchical SiO₂-QDs@SiO₂ nanostructures (QDs=CdTe, PbTe or PbS) has been developed. In the synthesis, 3-10 nm QDs covered by 1-2 nm SiO₂ shells were deposited onto the surface of SiO₂ nanobead carriers, resulting in the hierarchical SiO₂-QDs@SiO₂ nanostructures. The color-tunable hierarchical SiO₂-QDs@SiO₂ nanostructures perform excellent optical property with PL emission from green (CdTe) to Near-IR (PbS and PbTe) of the region. Moreover, the hierarchical SiO₂-QDs@SiO₂ nanostructures can be readily introduced to -COOH or -NH₂ active group. The hierarchical SiO₂-QDs@SiO₂-COOH nanostructures is available for covalent coupling to various biomolecules by cross-linking reaction, with the result that the SiO₂-QDs@SiO₂ nanostructures show promising potential applications in detecting fingerprint and imaging cells. This work sheds new light on the preparation of hierarchical SiO₂-QDs@SiO₂ nanostructures (QDs=CdTe, PbTe or PbS) and important applications in cell imaging and fingerprint detecting without being influenced by the multicolored environment.

7. Acknowledgment

This work was supported by the National Natural Science Foundation of China (Nos 51272235, 21301155); Zhejiang Provincial Natural Science Foundation of China (LR12E02001); Program for New Century Excellent Talents in University (NCET-13-0998); Program for Changjiang Scholars and Innovative Research Team in University (PCSIRT) and Open Project Program of State Key Laboratory of Inorganic Synthesis and Preparative Chemistry, Jilin University.

References

- [1] M. Bruchez, M. Moronne, P. Cin, S. Weiss and A. P. Alivisatos, *Science*, 1998, **281**, 2013-2016.
- [2] B. Dubertret, P. Skourides, D. J. Norris, V. Noireaux, A. H. Brivanlou and A. Libchaber. *Science*, 2002, **298**, 1759-1762.
- [3] H. B. Li, Y. L. Li and J. Cheng, *Chem. Mater.*, 2010, **22**, 2451-2457.
- [4] J. L. Zhao, J. Y. Zhang, C. Y. Jiang, J. Bohnenberger, T. Basché and A. J. Mews, *J. Appl. Phys.*, 2004, **96**, 3206-3210.
- [5] S. Nizamoglu, T. Ozel, E. Sari and H. V. Demir, *Nanotechnology*, 2007, **18**, 065709
- [6] H. Mattoussi, J. M. Mauro, E. R. Goldman, G. P. Anderson, V. C. Sundar, F. V. Mikulec and M. G. Bawendi, *J. Am. Chem. Soc.*, 2000, **122**, 12142-12150.
- [7] P. Alivisatos, *Nature Biotechnol.*, 2004, **22**, 47-52.
- [8] Y. Jun, J. H. Lee and J. Cheon, *Angew. Chem. Int. Ed.*, 2008, **47**, 5122-5135.
- [9] M. Rosso, A. Arafat, K. Schron, M. Giesbers and H. Zuilhof, *Langmuir*, 2008, **24**, 4007-4012.
- [10] E. M. Barea, M. Shalom, S. Giménez, I. Hod, I. Mora-Seró, A. Zaban and J. Bisquert, *J. Am. Chem. Soc.*, 2010, **132**, 6834-6389.
- [11] M. Darbandi, R. Thomann and T. Nann, *Chem. Mater.*, 2005, **17**, 5720-5725.
- [12] R. Koole, M. M. Schooneveld, J. Hilhorst, K. Castermans, D. P. Cormode, G. J. Strijkers, C. M. Donega, D. Vanmaekelbergh and A. W. Grifioen, *Bioconjugate Chem.*, 2008, **19**, 2471-2479
- [13] D. K. Yi, T. Selvan, S. S. Lee, G. C. Papaefthymiou, D. Kundaliya and J. Y. Ying, *J. Am. Chem. Soc.*, 2005, **127**, 4990-4991.
- [14] T. T. Tan, S. Selvan, T. L. Zhao, S. J. Gao and J. Y. Ying, *Chem. Mater.*, 2007, **19**, 3112-3117.
- [15] M. A. Correa-Duarte, M. Giersig and L. M. Liz-Marzan, *Chem. Phys. Lett.*, 1998, **286**, 497-501.
- [16] Y. Yang and M. Y. Gao, *Adv. Mater.*, 2005, **17**, 2354-2357.
- [17] P. Sharma, S. Brown, G. Walter, S. Santra and B. Moudgil, *Adv. Colloid Interface Sci.*, 2006, **123**, 471-485.
- [18] W. W. Yu, L. H. Qu, W. Z. Guo and X. G. Peng, *Chem. Mater.*, 2003, **15**, 2854-2860.
- [19] G. Konstantatos, I. Howard, A. Fischer, S. Hoogland, J. Clifford, E. Klem, L. Levina and E. H. Sargent, *Nature*, 2006, **442**, 180-183.
- [20] F. Rowell, K. Hudson and J. Seviour, *Analyst.*, 2009, **134**, 701-707.
- [21] R. N. Sanoj, P. C. Krishna, T. Hiroshi, V. N. Shantikumar and J. Rangasamy, *ACS Appl. Mater. Interfaces*, 2011, **3**, 3654-3665.
- [22] J. L. Duan, L. X. Song and J. H. Zhan, *Nano Research*, 2009, **1**, 61-68.
- [23] H. P. Klug and L. E. Alexander, *John Wiley & Sons New York*, 1954, **2**, 992.
- [24] K. Liu and L. Jiang, *Nanotoday*, 2011, **2**, 155-175.
- [25] L. Li, H. F. Qian, N. H. Fang and J. C. Ren, *J. Lumin.*, 2006, **116**, 59-66.
- [26] W. R. Algar and K. Susumu, *Anal. Chem.*, 2011, **83**, 8826-8837.
- [27] X. G. Peng and A. P. Alivisatos, *Nature.*, 2000, **404**, 59-61.
- [28] R. G. Xie, X. H. Zhong and T. Basché, *Adv. Mater.*, 2005, **12**, 2741-2745.

- [29] R. G. Xie, U. Kolb, J. X. Li, T. Basché and A. Mews, *J. Am. Chem. Soc.*, 2005, **127**, 7480-7488.
- [30] M. Rajamathi and P. V. Kamath, *J. Power Sources*, 1998, **70**, 118-121.
- [31] J. R. Millette, R. S. Brown and W. B. Hill, *Nature*, 2008, **18**, 20-30.
- [32] S. Oden and B. V. Hofsten, *Nature*, 1954, **173**, 449-450.
- [33] K. Karu and A. K. Jain, *Pattern Recognition*, 1996, **29**, 389-404.
- [34] P. Theys, Y. Turgis, A. Lepareux, G. Chevet and P. F. Ceccaldi, *Int.Crim. Police Rev.*, 1968, **217**, 106-108.
- [35] M. Sametband, I. Shweky, U. Banin, D. Mandler and J. Almog, *Chem. Commun.*, 2007, **0**, 1142-1144.
- [36] G. Carrot, D. Rutot-Houze, A. Pottier, P. Degee, J. Hilborn and P. Dubois, *Macromolecules*, 2002, **35**, 8400-8404.
- [37] L. Zhou, C. Gao, W. J. Xu, X. Wang and Y. H. Xu, *Biomacromolecules*, 2009, **10**, 1865-1874.
- [38] B. J. Theaker, K. E. Hudson and F. J. Rowell, *Forensic Sci. Int.*, 2008, **174**, 26-34.